Shukla, K. K., Levy, H. M., Ramirez, F., Marecek, J. F., McKeever, B., & Margossian, S. S. (1983) *Biochemistry 22*, 4822–4830.
Sleep, J. A., Hackney, D. D., & Boyer, P. D. (1980) *J. Biol. Chem. 255*, 4094–4099.
Spudich, J. A., & Watt, S. (1971) *J. Biol. Chem. 246*, 4866–4871.
Stadtman, E. R. (1957) *Methods Enzymol. 3*, 228–231.
Starr, R., & Offer, G. (1971) *FEBS Lett. 15*, 40–44.
Stein, L. A., Schwartz, R. P., Chock, B. P., & Eisenberg, E. (1979) *Biochemistry 18*, 3895–3908.
Taylor, R. S., & Weeds, A. G. (1976) *Biochem. J. 159*, 301–315.
Webb, M. R., & Trentham, D. R. (1981) *J. Biol. Chem. 256*, 10910–10916.
Weeds, A. G., & Taylor, R. S. (1975) *Nature (London) 257*, 54–56.
Weeds, A. G., & Pope, B. (1977) *J. Mol. Biol. 111*, 129–157.
Yazawa, M., & Yagi, K. (1978) *J. Biochem. (Tokyo) 84*, 1259–1265.
Young, D. M., Himmelfarb, S., & Harrington, W. F. (1964) *J. Biol. Chem. 239*, 2822–2829.

Activation of the Dynein Adenosinetriphosphatase by Microtubules†

Charlotte K. Omoto‡ and Kenneth A. Johnson*

Appendix: Kinetics of ATP-Induced Dissociation and Re-formation of the Microtubule–Dynein Complex

Kenneth A. Johnson

Department of Molecular and Cell Biology, The Pennsylvania State University, University Park, Pennsylvania 16802
Received June 3, 1985; Revised Manuscript Received September 12, 1985

ABSTRACT: Previous work has indicated that following the rapid adenosine 5′-triphosphate (ATP) induced dissociation of the microtubule–dynein complex, the rate-limiting step in the ATPase cycle is product release [Johnson, K. A. (1983) *J. Biol. Chem. 258*, 13825–13832], which occurs at a rate of approximately 2–6 s^{-1}. In this report we complete the analysis of the ATPase cycle by examining the effect of microtubules on the rate of product release. For these studies we used repolymerized *Tetrahymena* axonemal microtubules and microtubule-associated protein (MAP) free bovine brain microtubules which were shown to be free of any measurable ATPase activity. *Tetrahymena* 22S dynein bound to these microtubules predominantly by the ATP-sensitive site and at a rate giving an apparent second-order rate constant of (0.2–1) × 10^6 M^{-1} s^{-1}, which is 50-fold greater than the rate observed with brain microtubules containing MAPs. ATP induced the rapid dissociation of the microtubule–dynein complex with an apparent second-order rate constant vs. ATP concentration equal to 1.6 × 10^6 M^{-1} s^{-1}; this value is only slightly lower than that observed in the presence of MAPs. After the ATP-induced dissociation, the dynein reassociated with the microtubules following a lag period due to the time required to hydrolyze the ATP. The duration of the lag time for reassociation decreased with increasing microtubule concentration, suggesting that microtubules increased the rate of ATP turnover. Direct measurements at steady state showed that the specific activity of the dynein increased with increasing microtubule concentration. These data provide clear evidence for activation of the dynein ATPase by microtubules in solution by a mechanism in which the rebinding of the dynein–product intermediate to the microtubules [at a rate of (1.2–6) × 10^4 M^{-1} s^{-1}] enhances the rate of product release.

Previous work has established the first two steps of the microtubule–dynein ATPase according to Scheme I, where M represents a microtubule and D represents dynein. The binding of adenosine 5′-triphosphate (ATP)[1] (step 1) induces a rapid dissociation of dynein from the microtubule (step 2) which is followed by a slower hydrolysis reaction (step 3) (Porter & Johnson, 1983; Johnson, 1983). The rate-limiting step in the steady state in the absence of microtubules is the release of products (step 6), which occurs at a rate of 2–6 s^{-1}. This reaction is too slow to be part of the in vivo mechanochemical cycle because it cannot account for one ATP per active site per beat with flagellar beat frequencies of 30–60 Hz (Brokaw & Benedict, 1968; Gibbons & Gibbons, 1972). Accordingly, one might expect that microtubules bind to the dynein–product intermediate (D·ADP·P_i or D·ADP) and enhance the rate of product release.

Gibbons & Fronk (1979) showed that dynein was activated approximately 6-fold when it rebound to the axonemal lattice. Although these data strongly suggest that the ATPase rate

†Supported by National Institutes of Health Grants GM26726 (to K.A.J.) and GM33027 (to C.K.O.). K.A.J. was supported by an Established Investigatorship of the American Heart Association with funds contributed in part by the Pennsylvania Affiliate.
*Correspondence should be addressed to this author.
‡Present address: Program in Genetics and Cell Biology, Washington State University, Pullman, WA 99164-4350.

[1] Abbreviations: ATP, adenosine 5′-triphosphate; EGTA, ethylene glycol bis(β-aminoethyl ether)-*N,N,N′,N′*-tetraacetic acid; GTP, guanosine 5′-triphosphate; MAP, microtubule-associated protein; Me_2SO, dimethyl sulfoxide; PIPES, piperazine-*N,N′*-bis(2-ethanesulfonic acid); SDS, sodium dodecyl sulfate.

0006-2960/86/0425-0419$01.50/0

Scheme I

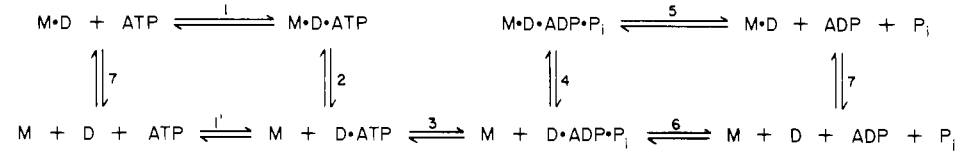

is activated by the ATP-sensitive interaction of the dynein with the B tubule, one could not exclude the possibility that binding by the structural site to the A tubule or binding to other axonemal components had altered that activity. Moreover, such a system with the dynein constrained within an axonemal lattice does not allow quantitation of the important kinetic parameters governing dynein binding and necessary to establish the pathway. To fully understand the basis for this activation and thereby establish the ATPase pathway, it is necessary to measure the rate of association of the microtubule–dynein complex in solution and to correlate that rate with the rate of ATP turnover as a function of microtubule concentration.

Until now, the failure to observe significant activation of the ATPase by microtubules could be understood in terms of the relatively fast rate of product release (k_6) and the slow rate of binding to microtubules (k_4 or k_7). To observe a significant contribution to the net turnover rate from this enhanced rate of release of products, the rate of microtubule binding to dynein must exceed the rate of product release from dynein. However, in previous experiments using bovine brain microtubules containing microtubule-associated proteins (MAPs), activation could not be detected due to the slow rate of dynein binding ($k_7 = 10^4$ M^{-1} s^{-1}) and the concentration of microtubules accessible in solution (10^{-4} M) (Johnson & Porter, 1982).

In this report, we examined the interaction of *Tetrahymena* 22S dynein with microtubules repolymerized from column-purified tubulin isolated from *Tetrahymena* axonemes or bovine brain microtubules. The microtubules made from column-purified, MAP-free tubulin were free of measurable ATPase activity, could be made at relatively high concentrations, and bound dynein at a rate sufficient to activate the ATPase.

Experimental Procedures

Dynein Preparation. Tetrahymena 22S dynein was obtained by high-salt extraction of *Tetrahymena* cilia and purified by DEAE-Sephacel chromatography and sucrose gradient sedimentation as previously described (Porter & Johnson, 1983a). This faster sedimenting dynein species isolated from *Tetrahymena* cilia was previously referred to as the 30S species on the basis of the original work of Gibbons (1965) but has recently been shown to sediment at 22 S (Clutter et al., 1985; D. Clutter et al., unpublished results). All assays were done in a buffer containing 50 mM PIPES, 4 mM $MgSO_4$, and 0.1 mM EGTA at pH 6.95.

Preparation of Microtubules. Bovine brain microtubules were prepared by three cycles of temperature-dependent polymerization and depolymerization (Borisy et al., 1974; Murphy & Hiebsch, 1979) and stored as frozen pellets. MAP-free brain microtubules were prepared by using a slight modification of the method of Borisy et al. (1974) as follows. Freshly thawed pellets of tubulin were carried through another cycle of temperature-dependent depolymerization and polymerization. After polymerization, the tubulin was depolymerized in PMG buffer (0.1 M PIPES, 0.1 mM $MgSO_4$, and 0.1 mM GTP, pH 6.6) with 0.19 M NaCl at a ratio of 3 mL of buffer per gram wet weight of pellet. The tubulin was then applied to a DEAE-Sephacel column equilibrated in the same buffer at a ratio of 3–4 mg of protein per milliliter of column. Tubulin was eluted with 0.5 M NaCl in PMG and dialyzed for 1 h against PMG plus 4 mM $MgSO_4$; 1 mM GTP and 7% Me_2SO (Himes et al., 1977) were added to the dialyzed tubulin solution, and the tubulin was polymerized by incubation at 30 °C for 30 min. The microtubules were pelleted at 18000 rpm (Sorvall ss-34) at 30 °C for 30 min. The pellet was resuspended in PMG with 4 mM $MgSO_4$ and 1 mM GTP, and microtubules were depolymerized by incubation on ice and then clarified by centrifugation at 4 °C and 18K rpm for 20 min. The supernatant was repolymerized by the addition of 7% Me_2SO at 30 °C for 30 min. Stock solutions of depolymerized tubulin were stored at −70 °C, repolymerized at 30 °C with 7% Me_2SO just before use, and stabilized by the addition of taxol at a concentration equal to the molar concentration of tubulin.

Tetrahymena axonemal tubulin was prepared in a manner similar to that of MAP-free microtubules using axonemal pellets after high-salt extraction of dynein. The tubulin was extracted by homogenizing the pellets in 0.19 M NaCl in PMG buffer with a Tissumizer (Tekmar Co., Cincinnati, OH, Model SDT-1810) at 50% setting on ice with 15-s bursts for a total of 1 min. The homogenate was centrifuged twice (18000 rpm, 30 min, Sorvall ss-34 rotor) to remove unsolubilized material, and the supernatant was loaded onto a DEAE-Sephacel column as described for MAP-free microtubules. The isolated tubulin was dialyzed and polymerized as described above, and then the first microtubule pellet was centrifuged after the addition of 1 mM ATP. The microtubules were cold-depolymerized, clarified, and repolymerized with 1 mM GTP and 7% Me_2SO at 30 °C. This two-step polymerization procedure and washing with 1 mM ATP were necessary to further reduce contaminating ATPase activity. For either microtubule preparation, no contaminating ATPase activities were detected over the time course of our steady-state ATPase assay with a limit of sensitivity of ~0.5% of the total ATP hydrolyzed in 10 min. Longer time course assays showed negligible activities in the range of 0.01–0.05 nmol/(mg·min).

Polymerized microtubules which were to be used in steady-state ATPase assays were centrifuged in the Beckman airfuge at top speed for 60 s and then resuspended in the appropriate concentration of buffer without Me_2SO. The highest concentration of Me_2SO in the stopped-flow association and reassociation experiments was 0.7% and 0.35%, respectively. One percent Me_2SO had no measurable effect on the dynein ATPase, and although higher concentrations of Me_2SO tested (up to 7%) had a slight inhibitory effect, we have not observed activation of the dynein ATPase at concentrations of Me_2SO used in our experiments.

Experiments are reported using repolymerized axonemal microtubules or MAP-free brain microtubules, where noted. All experiments were repeated with both types of microtubules, and essentially identical results were obtained with each source of tubulin.

Protein Determination. Dynein concentration was determined by absorbance measurements using an extinction coefficient at 280 nm of 0.97 cm^2/mg (Clutter et al., 1985; D. Clutter et al., unpublished results). In cases where a

turnover number per site is reported, we used a molecular weight of 750000 per site (Johnson, 1983; Shimizu & Johnson, 1983). Although a net mass of 1.95×10^6 daltons for the three-headed dynein has been obtained (Johnson & Wall, 1983), we believe that the active-site titrations more accurately reflect the concentration of active protein sites in our preparation by accounting for a small fraction of inactive protein. Tubulin concentration was determined by using the Bio-Rad micro protein assay with ovalbumin as the standard. Polymerized microtubules of undetermined length were used, and their concentration was expressed as the molar concentration of tubulin dimers using a molecular weight of 100000 (Ponstingl et al., 1981; Krauhs et al., 1981).

Transient Kinetics. Stopped-flow light-scattering measurements were done by monitoring the light scattering at 90° to the incident beam at a wavelength of 420 nm as previously described (Porter & Johnson, 1983b). All experiments were performed at 28 °C, and the reaction was initiated by mixing 100 μL of solution from each syringe. Concentrations are expressed as that after mixing. For association experiments, various concentrations of microtubules were mixed with dynein, and for each set of experiments, the ratio of microtubules to dynein was kept constant. The kinetics of association and ATP-induced dissociation of the microtubule–dynein complex were fit to a double or a single exponential, respectively, by the method of moments (Dyson & Isenberg, 1971). That is, the change in light scattering was fit to an equation of the form $Y = Ae^{-k_1 t} + Be^{-k_2 t} + C$ in the case of a double exponential or $Y = Ae^{-k_1 t} + C$ in the case of a single exponential.

For reassociation experiments, a preformed microtubule–dynein complex was mixed with a buffer containing ATP or ATP and microtubules. Since the different concentrations of microtubules dramatically changed the absolute values of light scattering, the plots were normalized during the curve-fitting process for the data shown in Figure 5. The time dependence of the light-scattering change due to the dissociation and reassociation of the microtubule–dynein complex was simulated by numerical integration of the differential equations describing the process using a KINSIM (kinetic simulation) program generously provided to us by Carl Frieden (Washington University, St. Louis, MO). Details of the equations and the method are provided in the Appendix.

ATPase Assays. Routine ATPase measurements were performed by using the malachite green phosphate assay (Lanzetta et al., 1979). In some cases, steady-state ATPase activity at 1 mM ATP was measured by using [γ-^{32}P]ATP using charcoal columns to adsorb unreacted ATP as described by Johnson (1983). For assay of ATPase activity at low ATP concentrations (Figure 7), a coupled assay system was employed by using phosphoenolpyruvate with pyruvate kinase to regenerate the ATP, and lactate dehydrogenase with NADH to provide an optical signal by monitoring the disappearance of NADH at 340 nm.

The analytical solution to the steady-state rate equation for microtubule activation of the ATPase at saturating ATP concentration was obtained for Scheme I by using two simplifications. Because the dissociation of dynein from the microtubule is very fast following ATP binding, step 2 was deleted, thereby making dissociation coincident with ATP binding. Similarly, product release was assumed to occur instantaneously following microtubule binding to the dynein–products intermediate. This latter assumption is used only because the small degree of curvature in the plot (Figure 6) does not provide enough information to specify a constant for step 5. The constant k_4 should therefore be considered only as an apparent second-order rate constant for the effect of microtubules in stimulating the release of products from dynein and may include terms from steps 4 and 5. The simplified scheme leads to the equation:

$$v = (k_1 k_3 k_{1'}[\mathrm{A}]^2 + k_1 k_3 k_7)(k_4[\mathrm{M}] + k_6)/\mathrm{den}$$

where the denominator (den) equals

$$\mathrm{den} = k_1 k_{1'}(k_3 + k_{-3} + k_6)[\mathrm{A}]^2 + k_1 k_7(k_3 + k_{-3} + k_6) \times [\mathrm{A}][\mathrm{M}] + k_3 k_4 k_7[\mathrm{M}]^2 + k_{1'} k_3 k_4[\mathrm{A}][\mathrm{M}] + k_1 k_4 k_7[\mathrm{A}][\mathrm{M}]^2 + k_1 k_{1'} k_4[\mathrm{A}]^2[\mathrm{M}] + k_3 k_6 k_7[\mathrm{M}] + k_1 k_3 k_6[\mathrm{A}] \quad (1)$$

and [A] represents the ATP concentration and [M] represents the steady-state microtubule concentration.

Equation 1 was used to calculate the curve in Figure 6 with the following rate constants: $k_1 = k_{1'} = 1.5 \times 10^6$ M^{-1} s^{-1}, $k_3 = 50$ s^{-1}, $k_{-3} = 5$ s^{-1}, $k_4 = 1.2 \times 10^4$ M^{-1} s^{-1}, $k_6 = 1.7$ s^{-1}, $k_7 = 1.0 \times 10^6$ M^{-1} s^{-1} (these data were not sensitive to the choice of the rate constant k_7 because there is no free dynein at saturating ATP concentrations and a value of $k_7 = 0.1 \times 10^6$ M^{-1} s^{-1} fit the data equally well). The rate constants for ATP binding (k_1 and $k_{1'}$), ATP hydrolysis (k_3), ATP synthesis (k_{-3}), and the binding of free dynein to the microtubules (k_7) were based upon independent measurements (Johnson, 1983; this report). The only parameters used to fit the data in Figure 6 were the rate of product release from free dynein (k_6), which was obtained from the intercept at zero microtubule concentration, and the rate of binding microtubules to the dynein–products complex (k_4), which was obtained as the fit to the slope of the curve. The slight degree of curvature in the plot would be due to the rate-limiting hydrolysis step according to the model, but there is no evidence to indicate that this must be the case.

Quantitation of Binding. The binding of dynein was quantitated by gel electrophoresis of material that cosedimented with microtubules. Microtubules were incubated with dynein in 100-μL aliquots for 20 min. They were then centrifuged at maximum speed for 60 s in the Beckman airfuge, either with or without the addition of 1 mM ATP and 0.1 mM sodium orthovanadate. Supernatants were withdrawn and mixed with gel sample buffer. Pellets were resuspended in 50 μL of gel sample buffer. Volumes were adjusted such that equivalent proportions of supernatant and pellet fractions were analyzed by SDS–polyacrylamide gel electrophoresis to obtain a semiquantitative measurement of the amount of dynein that cosedimented with microtubules.

RESULTS

Association of Dynein with Repolymerized Tubulin. We first examined the interaction of dynein with repolymerized microtubules by quantitating the binding and ATP-induced dissociation. Panels A and C of Figure 1 show the complex formed between *Tetrahymena* 22S dynein and repolymerized axonemal microtubules and MAP-free brain microtubules, respectively. In each case, dynein bound with the characteristic 24-nm repeat, and the addition of ATP to the microtubule–dynein complex led to the complete dissociation of dynein from the microtubules (Figure 1B,D). Thus, as reported previously with MAP-containing bovine brain microtubules, the dynein associates with each microtubule lattice in an ATP-sensitive manner.

The degree of association and the ATP-induced dissociation were quantitated by polyacrylamide gel electrophoresis of the protein that cosedimented with microtubules. Figure 2 shows a gel of the supernatant and pellet formed after sedimentation in the absence or presence of ATP using MAP-free brain

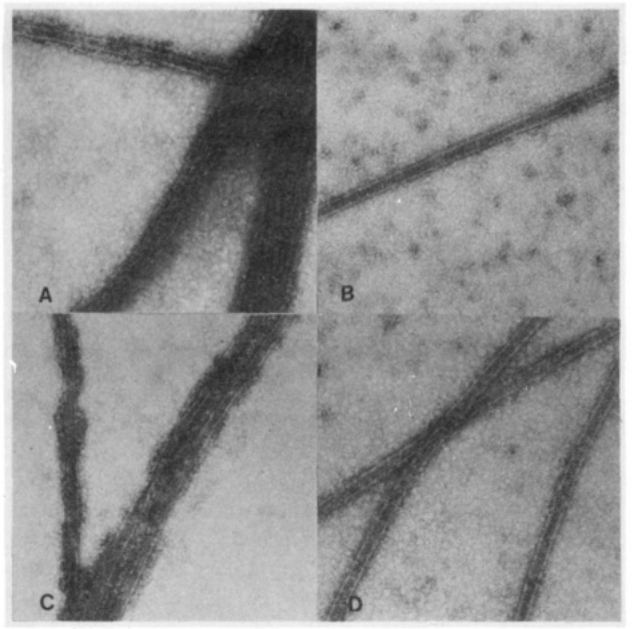

FIGURE 1: Association and dissociation of *Tetrahymena* 22S dynein with microtubules. Electron micrographs show 22S dynein combined with MAP-free bovine brain microtubules (A and B) and *Tetrahymena* axonemal microtubules (C and D). The images on the right (B and D) show the dissociation of dynein after addition of 1 mM ATP and 0.1 mM orthovanadate.

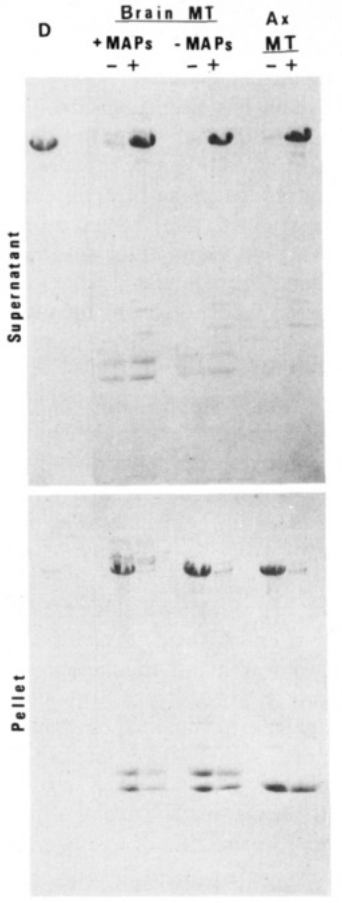

FIGURE 2: Polyacrylamide gel showing the cosedimentation of 22S dynein with microtubules. Supernatants are displayed on the upper panel and pellets on the lower. Microtubules used were bovine brain microtubules (+MAPs), MAP-free bovine brain microtubules (−MAPs), or repolymerized axonemal microtubules (Ax. MT). Plus (+) or minus (−) refers to the presence or absence of 1 mM ATP and 0.1 mM orthovanadate which causes the dissociation of the microtubule–dynein complex.

microtubules and repolymerized exonemal microtubules. The data indicate that a large fraction (>95%) of the dynein bound in the absence of ATP and dissociated from the microtubules in the presence of ATP for each source of tubulin. Therefore, in each case, the binding of dynein mimics the association of dynein with the B tubule of the outer doublet. Although the basis for this specificity of binding is not understood, it provides the appropriate model system to examine the reactions involved in the coupling of ATP hydrolysis to the dynein–microtubule cross-bridge interaction.

We examined the time course of formation of the microtubule–dynein complex by stopped-flow light-scattering methods. An example showing the increase in light-scattering intensity after dynein is mixed with microtubules is given in Figure 3A. The formation of the microtubule–dynein complex followed a double exponential with the two rates differing by a factor of 5. The microtubule concentration dependence of the rates of the fast and the slow phases of the reaction is shown in Figure 3B. The slope of each line defines the apparent second-order rate constant for the fast and slow phases to be approximately 1×10^6 and 0.2×10^6 M^{-1} s^{-1}, respectively. The amplitude of the fast phase was approximately equal to that of the slow phase at each concentration of microtubules used. Similar results were seen with MAP-containing microtubules (Porter, 1982; Johnson & Porter, 1982), but the rates of association were approximately 50-fold slower than the results presented here in the absence of MAPs. The basis for the biphasic binding in either case and the significance of the apparent inhibition of binding by MAPs are not understood and will be the subjects of further study. The faster rate of association in the absence of MAPs is important for the present work in terms of the ability of microtubules to activate the dynein by binding at a rate that exceeds the rate of spontaneous product release.

The time course of ATP-induced dissociation of the dynein–microtubule complex is shown in Figure 4. The light-scattering change follows a single exponential as described previously for MAP-containing microtubules. The rate of dissociation was a linear function of ATP concentration with an apparent second-order rate constant of 1.6×10^6 M^{-1} s^{-1}, which is only slightly smaller than the rate constant reported previously in the presence of MAPs (Porter & Johnson, 1983). Thus, the rate of ATP-induced dissociation of the microtubule–dynein complex was largely unaffected by the presence or absence of MAPs or the source of the tubulin.

Reassociation of the Microtubule–Dynein Complex. In order to estimate the rate of binding of microtubules to the dynein–products complex, we have examined the kinetics of the rebinding of dynein to the microtubule following the addition of ATP to a microtubule–dynein complex. A preformed microtubule–dynein complex was mixed in the stopped-flow apparatus with a low concentration of ATP (20 μM), and the change in light scattering was recorded to get the results shown in Figure 5. There was an initial rapid decrease in light scattering due to the dissociation of the microtubule–dynein complex during the first 500 ms after mixing. Over the period of the next several seconds, the light scattering increased and returned to the original level. Because the amplitude of the regain in light scattering equaled the amplitude of the dissociation, the complex quantitatively re-formed. Moreover, because a second addition of ATP again induced the dissociation of the dynein from the microtubule (data not shown), the complex that was re-formed upon the depletion of ATP still mimicked the association of dynein with the B microtubule.

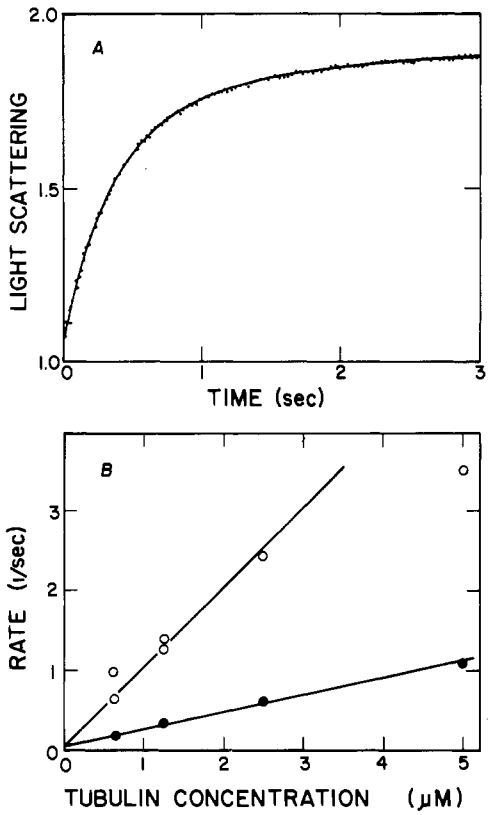

FIGURE 3: (A) Kinetics of association of dynein with microtubules. Time dependence of the light-scattering change showing the binding of 22S dynein with repolymerized *Tetrahymena* axonemal microtubules. The ratio of 22S dynein to microtubules, 0.3:1 (mg/mg), provides a 10-fold molar excess of tubulin sites. The fit to a double exponential shown by the solid line gave rates of 3.5 and 1.1 s^{-1}. The fast phase accounted for 58% of the signal amplitude. (B) Rates of association of dynein with microtubules. Rates of formation of the microtubule–dynein complex are plotted as a function of microtubule concentration. Rates of association for the slow phase (●) and fast phase (○) of the double-exponential fit were determined as shown in Figure 3A. Slopes of the two lines give the apparent second-order rate constants of 1×10^6 and 0.2×10^6 M^{-1} s^{-1} for the fast and slow phases, respectively. The relative amplitudes of the fast and slow phases were independent of microtubule concentration.

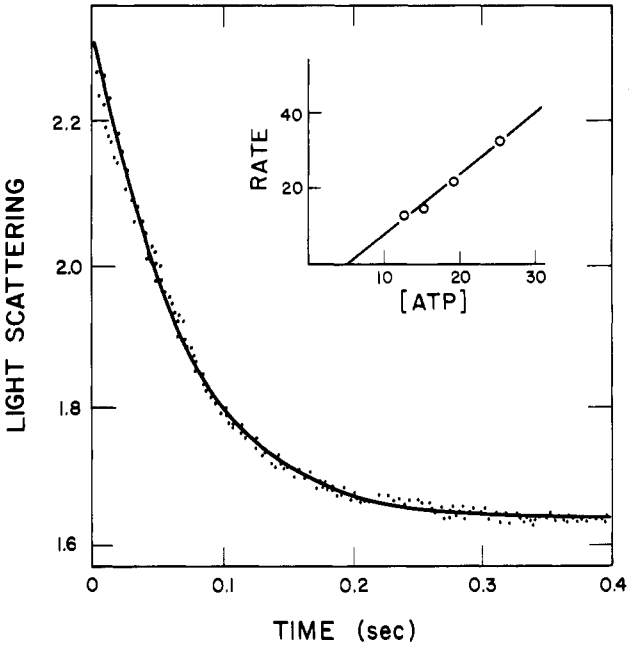

FIGURE 4: Time dependence of ATP-induced dissociation of the microtubule–dynein complex. Light-scattering intensity (arbitrary units) is shown as a function of time after the addition of ATP (15 μM) with a microtubule–dynein complex formed with repolymerized axonemal tubules. The fit to a single exponential (smooth line) gave a rate of 14.5 s^{-1}. The insert shows the rate (s^{-1}) vs. ATP concentration (micromolar) with a slope defining a second-order rate constant for ATP binding of 1.6×10^6 M^{-1} s^{-1}.

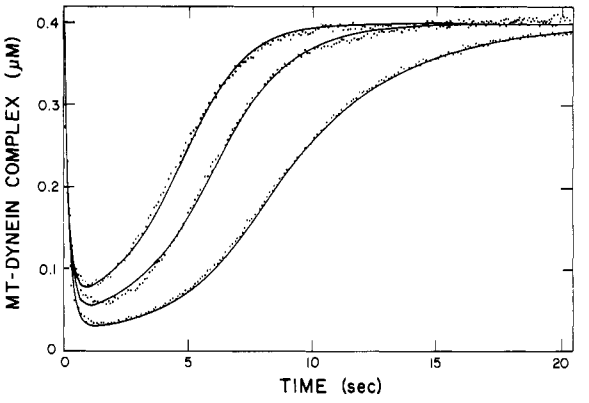

FIGURE 5: Kinetics of reassociation of the microtubule–dynein complex. The time dependence of the light-scattering change shows a rapid dissociation and slower reassociation of 22S dynein following the addition of ATP to a preformed dynein–microtubule complex. The three plots were obtained with the same concentrations of dynein (0.3 mg/mL ≃ 0.4 μM sites) and ATP (20 μM at the start of the time course) and varying concentrations of MAP-free bovine brain microtubules; the curves from left to right were obtained at 9, 6, and 3 μM tubulin, respectively. The three curves were normalized because the different tubulin concentrations contributed a variable background light-scattering intensity. The amplitudes of the light-scattering changes were 58%, 36%, and 29%, at 3, 6, and 9 μM tubulin, respectively, calculated relative to the minimum in the signal. The smooth lines were calculated by using a single set of rate constants as described in the Appendix. Similar results were obtained with repolymerized axonemal microtubules.

The time dependence of the re-formation of the microtubule–dynein complex following the addition of ATP is a function of the ATPase and reassociation rates such that the lag time in rebinding provides an approximate measure of the ATPase rate. The shorter lag time observed at higher microtubule concentrations suggests that the microtubules activated the ATPase. Moreover, the increase in the observed rate of reassociation with increasing microtubule concentration also suggests that the microtubules activate the dynein ATPase by binding to the dynein–ADP–P_i intermediate to enhance the rate of product release. This conclusion was confirmed by simulation of the kinetics; the smooth lines drawn in Figure 5 were calculated by using one set of kinetic constants as described in the Appendix.

Activation of Steady-State ATPase Activity. The steady-state ATPase activity at 1 mM MgATP was directly measured as a function of microtubule concentration. Dynein was mixed with [γ-^{32}P]ATP and various concentrations of microtubules, and the rate of ATP hydrolysis in solution was determined. Figure 6 shows the specific activity of the dynein as a function of microtubule concentration, expressed as the molar concentration of tubulin dimers. In this experiment, there was a 5-fold increase in specific activity up to a concentration of 0.5 mM tubulin (50 mg/mL), and this is representative of the results of several experiments showing 3–10-fold activation. The principal source of variation in the degree of activation appears to be the variation in the basal activity of the dynein in the absence of microtubules which ranged between 0.15 and 0.38 μmol/(mg·min) in various preparations.

The slight degree of curvature in the line drawn in Figure 6 is due to a rate-limiting hydrolysis step at saturating microtubules in the model calculations as described under Ex-

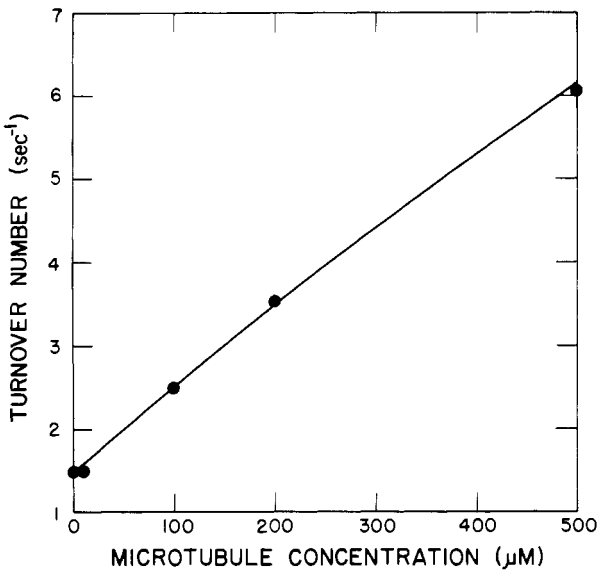

FIGURE 6: Activation of the dynein steady-state ATPase activity by microtubules. Specific activity of 22S dynein at 1 mM ATP is shown as a function of concentration of repolymerized *Tetrahymena* axonemal microtubules. The steady-state ATPase activity was measured from the time dependence of release of phosphate using [γ-^{32}P]ATP. The line was calculated according to the complete analytical solution to Scheme I as described under Experimental Procedures.

perimental Procedures. Alternatively, there could be a rate-limiting step involving the release of products from the ternary complex. However, the degree of curvature is slight and somewhat variable in various experiments and therefore does not warrant further refinements in attempts to fit the data at this time. Accordingly, no information is available to define the rate-limiting step at saturating microtubule concentration. The limiting slope of the line at low tubulin concentration defines the apparent second-order rate constant for the binding of the dynein–products complex to a microtubule to be 1.2×10^4 M^{-1} s^{-1}.

Attempts to fit the kinetics of reassociation of the microtubule–dynein complex (Figure 5 and Appendix) using a single-site model required a rate constant of approximately 2.5×10^6 M^{-1} s^{-1}, which is 200 times larger than the value measured at saturating ATP concentration (Figure 6). We reasoned that this discrepancy may be due to the multiple dynein heads (Shimizu & Johnson, 1983), leading to a further activation of the ATPase at low concentrations of ATP. At low concentrations of ATP, it seemed probable that the rate of dissociation of all three dynein heads would be sufficiently slow to allow the tethering of dynein to a microtubule by one or more of its heads and thus any dissociated head would see a high local concentration of tubulin (see the Appendix). This explanation appeared reasonable because the concentration of ATP varied throughout the time course shown in Figure 5 from 20 μM at the start of the reaction to zero at the end.

In order directly to test this postulate, we examined the effect of a low concentration of microtubules (5 μM) on the rate of steady-state ATP turnover at low concentrations of ATP. This microtubule concentration is insufficient to activate the ATPase at saturating ATP concentration (Figure 6). Figure 7A shows the rate vs. ATP concentration in the presence and absence of repolymerized axonemal microtubules. Figure 7B shows the data graphed as the ratio of activities in the presence and absence of microtubules and extending to higher ATP concentrations. The results clearly demonstrate that there is a 2-fold activation near 1 μM ATP that diminishes as the ATP concentration is raised. This result substantiates

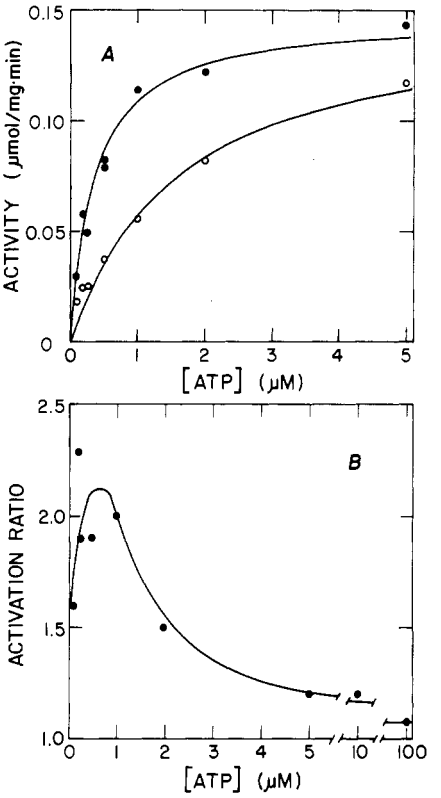

FIGURE 7: Microtubule-dependent activation of dynein at low ATP concentration. (A) The specific activity of 22S dynein is shown as a function of ATP concentration in the presence (●) and absence (○) of 5 μM repolymerized axonemal tubulin. The ATP concentration was maintained, and the steady-state ATPase was measured with a coupled enzyme assay system comprised of pyruvate kinase and lactate dehydrogenase. The fits to a hyperbola are shown by the solid lines using a V_{max} = 0.148 μmol/(mg·min) for both curves and K_m = 0.36 and 1.54 μM, respectively, in the presence and absence of microtubules. (B) The ratio of specific activities of 22S dynein in the presence to that in the absence of microtubules is shown as a function of ATP concentration.

our quantitative interpretation of the reassociation kinetics given in Figure 5 and described in the Appendix. More importantly, regardless of the complications introduced by the multiple dynein heads, the data demonstrate that at both high and low ATP concentration, microtubules activate the steady-state turnover of ATP by enhancing the rate of product release.

Discussion

In this report, we describe the first quantitative demonstration of activation of the dynein ATPase by microtubules in solution. Two independent experiments provided evidence for activation; direct measurement of the ATPase activity as a function of increasing microtubule concentration and analysis of the kinetics of reassociation of the microtubule–dynein complex after ATP-induced dissociation. Moreover, these observations together with our previous analysis of the ATPase cycle indicate that microtubules bind to a dynein–products complex to increase the rate of product release according to Scheme II. This pathway is supported by the observation that microtubules can enhance the rate of product release (Figure 6). Furthermore, the decrease in the lag time in the reassociation kinetics with increasing microtubule concentration suggested that a faster rate of binding was sufficient for the dynein ATPase to be activated by microtubules (Figure 5). As described in the Appendix, the data can be adequately fit by using a rate constant of $k_4 = (1.2–6) \times 10^4$ M^{-1} s^{-1} for the

Scheme II

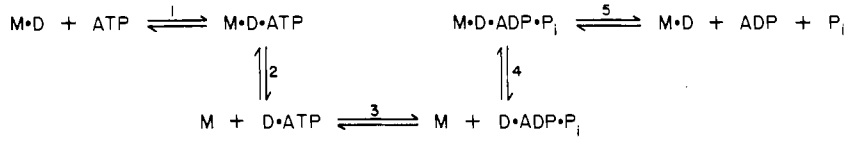

rate of binding of the dynein–products complex to the microtubule. Although the release of products from the ternary M•D•ADP•P_i complex (step 5) may be rate limiting at saturating microtubule concentrations, we have no evidence regarding the magnitude of this rate constant.

It is possible that phosphate release is more rapid and ADP release is the rate-limiting step during the steady state (E. L. F. Holzbaur and K. A. Johnson, unpublished results). If this proves to be the case, the current data may indicate that microtubules bind to a dynein–ADP intermediate to enhance the turnover rate.

The concentration of microtubules required to observe significant activation in solution is rather high but not unreasonable with respect to the concentration of tubulin in the cilium. The average concentration of tubulin in the axoneme is approximately 1 mM, and the local concentration near a dynein head may be even larger, perhaps 5 mM. Moreover, the 5-fold activation seen at 0.5 mM tubulin is commensurate with the 6-fold activation observed by Gibbons & Fronk (1979) following the reassociation of dynein at sites within the axonemal lattice.

There have been several other reports of activation of the dynein ATPase by microtubules or tubulin (Telzer & Haimo, 1981; Otokawa, 1972; Hoshino, 1976). However, in these cases, the cause of the reported activation was not clear. For example, Hoshino (1976) saw only a modest enhancing effect of microtubules above pH 9 where the activity of the dynein was beginning to decrease. Telzer & Haimo (1981) reported a higher apparent specific activity in dynein that cosedimented with microtubules; however, because they had separated the mixture of bound and unbound dynein, they could not eliminate the possibility that the binding to microtubules had simply selected a subpopulation of active from inactive dynein in solution.

The key to the observed activation of dynein by microtubules in solution appears to be the removal of the microtubule-associated proteins which slow the rate of dynein binding by approximately 50-fold. It is significant that once the MAPs were removed, tubulin isolated either from bovine brain or from *Tetrahymena* axonemes interacted with dynein in a similar way. In each case, the *Tetrahymena* 22S dynein bound to the microtubules with a 24-nm linear repeat and in an ATP-sensitive manner. The rate of dissociation of the dynein from the microtubules was a linear function of the ATP concentration with an apparent second-order rate constant of 1.6×10^6 M^{-1} s^{-1}. This observation provides an important confirmation of a rapid ATP binding induced dissociation step using axonemal microtubules and may reflect the conservation of important binding sites on the microtubule surface lattice.

The effect of MAPs in inhibiting the rate of dynein binding to microtubules is rather large in magnitude and has potential physiological significance for cytoplasmic dynein. However, this question cannot be addressed using our heterologous system consisting of ciliary dynein and brain MAPs. For the present study, the much faster rate of binding is significant in that the MAP-free microtubules bind to the dynein at a rate sufficient to alter the lifetime of the dynein–products intermediate.

One should note that the estimated rate of binding of the dynein–products complex to microtubules (1.2×10^4 M^{-1} s^{-1}) is 2 orders of magnitude slower than the measured rate of binding of free dynein to microtubules [$(0.2–1) \times 10^6$ M^{-1} s^{-1}]. A similar situation exists in the case of actomyosin (Taylor, 1979) and contributes to the weaker binding of the myosin–nucleotide complex to actin relative to the rigor complex (Greene et al., 1983). In the case of dynein and microtubules, the present evidence indicates that MAPs may inhibit the binding of dynein or dynein–products to the microtubules by a similar amount (50–100-fold): In our previous measurements, the rate of reassociation of the dynein–products intermediate with MAP-containing microtubules was much slower than that reported here, and increasing the microtubule concentration did not shorten the lag time in the reassociation kinetics (Porter, 1982).

To fit the reassociation kinetics (Figure 5), it was necessary to include reactions involving all three dynein heads similar to those previously suggested (Shimizu & Johnson, 1983). As described in the Appendix, the multiple dynein heads lead to significant activation of the ATPase at low microtubule concentrations due to the transient tethering of the dynein to the microtubule by one of the three heads. This activation is significant only at low ATP concentration but does not require a high concentration of microtubules (see Appendix). This explains the apparent discrepancy in that no measurable activation was seen at 20 μM tubulin and 1 mM ATP (Figure 6) whereas the reassociation kinetics (Figure 5) implied significant activation at 3–9 μM tubulin in experiments where the ATP concentration varied from 20 μM at the start of the time course to zero at the end. Preliminary data (Figure 7) based upon direct measurement of the steady-state ATPase support this interpretation by showing that dynein can be activated by low concentrations of tubulin ($\sim$5 μM) at ATP concentrations of less than 20 μM, and we are currently working to more fully quantitate this reaction. Moreover, a similar activation was recently described for actomyosin at low ATP concentrations (Hackney & Clark, 1984).

The reason for the double-exponential time course for the association of the dynein with microtubules is not understood. The simplest explanation is that there exists two populations of dynein such that 60% of the molecules bind 5-fold faster than the remaining 40% of the dynein; however, there is no other evidence to support the suggestion of heterogeneity in this preparation. Models based upon a two-step association reaction such as the association of dynein followed by the cross-bridging of microtubules, or two rates of binding by a homogeneous preparation, are not consistent with the observed concentration dependence of the rates and amplitudes (Figure 3B).

Our observations provide clear evidence that the mechanism of activation of dynein reported here involves the rebinding of a dynein–product intermediate to microtubules to enhance the rate of release of products. The release of products is presumably coupled to the important changes in cross-bridge conformation that are responsible for movement. Moreover, as the rate-limiting step in the cycle, this is a likely site for regulation. The current work provides the methods and the background with which to begin a rigorous analysis of regulation of the dynein ATPase cycle.

ACKNOWLEDGMENTS

We thank Anita Sgrignoli for her assistance in performing the ATPase assays at low ATP concentration and Chuck Seldon for suggesting the methods to prepare microtubules at high concentrations.

Registry No. ATPase, 9000-83-3.

REFERENCES

Borisy, G. G., Olmsted, J. B., Marcum, J. M., & Allen, C. (1974) *Fed. Proc., Fed. Am. Soc. Exp. Biol. 33*, 167–174.

Brokaw, C. J., & Benedict, B. (1968) *Arch. Biochem. Biophys. 125*, 770–778.

Clutter, D., Stimpson, D., Bloomfield, V., & Johnson, K. A. (1985) *J. Cell Biol. 97*, 197a.

Dyson, R. D., & Isenberg, I. (1971) *Biochemistry 10*, 3233–3241.

Gibbons, B. H., & Gibbons, I. R. (1972) *J. Cell Biol. 54*, 75–97.

Gibbons, I. R. (1965) *Arch. Biol. 76*, 317–352.

Gibbons, I. R., & Fronk, E. (1972) *J. Cell Biol. 54*, 365–381.

Gibbons, I. R., & Fronk, E. (1979) *J. Biol. Chem. 254*, 187–196.

Greene, L. E., Sellers, J. E., Eisenberg, E., & Adelstein, R. S. (1983) *Biochemistry 22*, 530–535.

Hackney, D., & Clark, P. (1984) *Proc. Natl. Acad. Sci. U.S.A. 81*, 5345–5349.

Himes, R. H., Burton, P. R., & Gaito, J. M. (1977) *J. Biol. Chem. 252*, 6222–6228.

Hoshino, M. (1976) *Biochim. Biophys. Acta 462*, 49–62.

Johnson, K. A. (1983) *J. Biol. Chem. 258*, 13825–13832.

Johnson, K. A., & Porter, M. E. (1982) *Cell Motil., Suppl. 1*, 101–106.

Johnson, K. A., & Wall, J. S. (1983) *J. Cell Biol. 96*, 669–678.

Krauhs, E., Little, M., Kempf, T., Hofer-Warbinek, R., Ade, W., & Ponstingl, H. (1981) *Proc. Natl. Acad. Sci. U.S.A. 78*, 4156–4160.

Lanzetta, P. A., Alvarez, L. J., Reinach, P. S., & Candia, O. A. (1979) *Anal. Biochem. 100*, 95–97.

Murphy, D. B., & Hiebsch, R. R. (1979) *Anal. Biochem. 96*, 225–235.

Otokawa, M. (1972) *Biochim. Biophys. Acta 275*, 464–466.

Ponstingl, H., Krauhs, E., Little, M., & Kempf, T. (1981) *Proc. Natl. Acad. Sci. U.S.A. 78*, 2725–2761.

Porter, M. E. (1982) Ph.D. Thesis, University of Pennsylvania, Philadelphia, PA.

Porter, M. E., & Johnson, K. A. (1983a) *J. Biol. Chem. 258*, 6575–6581.

Porter, M. E., & Johnson, K. A. (1983b) *J. Biol. Chem. 258*, 6582–6587.

Shimizu, T., & Johnson, K. A. (1983) *J. Biol. Chem. 258*, 13841–13846.

Taylor, E. W. (1979) *CRC Crit. Rev. Biochem. 6*, 103–164.

Telzer, B. R., & Haimo, L. T. (1981) *J. Cell Biol. 89*, 373–378.

APPENDIX: KINETICS OF ATP-INDUCED DISSOCIATION AND RE-FORMATION OF THE MICROTUBULE–DYNEIN COMPLEX

The kinetics of dissociation and re-formation of the microtubule–dynein complex were modeled on the basis of a three-headed dynein according to the pathways shown in Figure A1 and Table AI. Although the model appears rather complex, information from several experiments was used to constrain the choices for various rate constants. ATP binding (steps 1–3) must give a net rate of ATP-induced dissociation of dynein from the microtubule that was consistent with the observed rate constant of 1.6×10^6 M^{-1} s^{-1}, and the rate of ATP binding to the free dynein (steps 4–6) was assumed to be the same. The rate of binding free dynein to a microtubule (step 12) was defined to be in the range of $(0.2–1.0) \times 10^6$ M^{-1} s^{-1} on the basis of direct measurement of this reaction. The rate of product release from free dynein (steps 9–11) was determined by the rate of steady-state turnover in the absence of microtubules (3 s^{-1}). Thus, the only parameters that were varied to fit the time course were the rate constant for binding dynein–nucleotide intermediates to the microtubule (steps 13–15) and the rate of rebinding a dynein head to the microtubule in the partially dissociated states (steps 7 and 8).

The time course of the reaction was simulated by numerical integration of the equations using the KINSIM program (Barshop et al., 1983) generously provided to us by Carl Frieden (Washington University, St. Louis, MO) which performs numerical integration based upon Gear's method. The scheme given in Figure A1 led to the elementary reactions shown in Table AI which served as the input to the simulation routine. The signal observed as light scattering from the dynein–microtubule complex was assumed to represent the summation of all bound states: $MD + MDA + MDA_2$.

The curves shown in Figure 5 of the text (Omoto & Johnson, 1986) were calculated by using the rate constants given in Table AI with a starting ATP concentration of 20 μM, a dynein concentration of 0.4 μM, and microtubule concentrations of 3, 6, and 9 μM. The observation that all three curves can be mimicked by one set of rate constants increases ones confidence in the validity of the fit. The essence of the model is that it suggests that at low ATP concentration, there is a significant population of partially dissociated dynein and that in this state, the close proximity of the dissociated head to the microtubule leads to activation of the rate of product release. The fit to the data suggests that the effective local concentration of microtubules around a dissociated head is approximately 0.5 mM, calculated as the ratio of the rate of rebinding the head (33 s^{-1}) to the second-order rate constant for the rate of rebinding a completely dissociated dynein (0.06×10^6 M^{-1} s^{-1}).

It is still likely that the set of constants chosen does not represent a unique fit. The fitting procedure was constrained by specifying that all of the steps involving the different heads have the same rate constant and this may not be the case. In particular, if different values for the rates of ATP binding to the three heads were used, a similar curve could be obtained by adjusting the rates of product release from the heads in the partially dissociated dynein.

ATP binding occurs sequentially in the diagram, but no defined sequence or differences in the heads were assumed; rather, rate constants were simply chosen for the first, second, and third heads to be dissociated. Accordingly differences in the rate constants might simply reflect differences in the probability of binding ATP to one of the three heads depending upon current occupancy or might reflect cooperativity. For example, if all three heads were identical, one might expect that the rate constants for binding ATP to the first head might be 3-fold greater than those for binding the last head. Alternatively, if the rate constants increase from the first to the last head, this would necessarily imply cooperativity because otherwise the head to most rapidly bind ATP would be first.

One should note that the hydrolysis step is not explicitly included in the model and both enzyme–ATP and enzyme–ADP–P_i complexes are expressed as the total enzyme–nucleotide complexes. Therefore, the rate constants for steps involving the enzyme–nucleotide complex include terms due

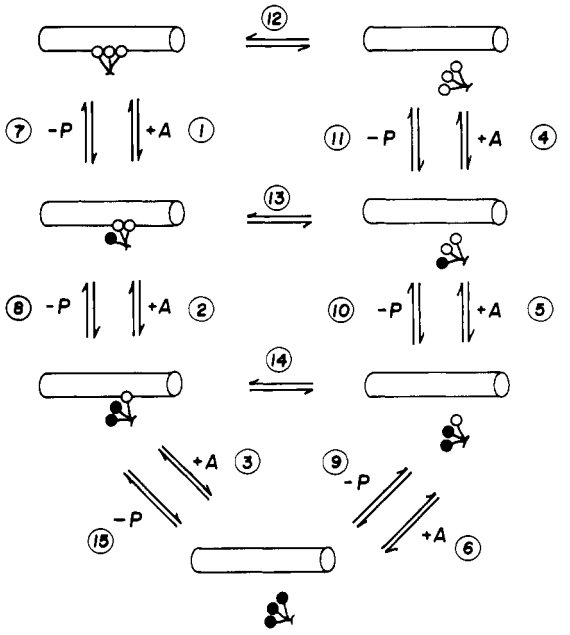

FIGURE A1: Intermediate states in the ATP-induced dissociation of the microtubule–dynein complex. The figure shows pathways for the ATP-induced dissociation and recombination of the microtubule–dynein complex and ATP binding and product release by each intermediate. The solid circles represent dynein heads with nucleotide bound. Each step is allowed to be reversible. For example, step 1 could reverse with the rebinding of the dissociated head and the release of ATP (k_{-1}) or with the release of products (k_7). The numbering of the steps corresponds to that given in Table AI.

Table A1: Kinetic Steps and Constants Used in Simulation[a]

reaction	kinetic constants
ATP Binding Steps	
$MD + A \rightleftharpoons MDA$	$k_1 = 1.5\ \mu M^{-1}\ s^{-1}$, $k_{-1} = 0.1\ s^{-1}$
$MDA + A \rightleftharpoons MDA_2$	$k_2 = 1.5\ \mu M^{-1}\ s^{-1}$, $k_{-2} = 0.1\ s^{-1}$
$MDA_2 + A \rightleftharpoons M + DA_3$	$k_3 = 1.5\ \mu M^{-1}\ s^{-1}$, $k_{-3} = 0.1\ s^{-1}$
$D + A \rightleftharpoons DA$	$k_4 = 1.5\ \mu M^{-1}\ s^{-1}$, $k_{-4} = 0.1\ s^{-1}$
$DA + A \rightleftharpoons DA_2$	$k_5 = 1.5\ \mu M^{-1}\ s^{-1}$, $k_{-5} = 0.1\ s^{-1}$
$DA_2 + A \rightleftharpoons DA_3$	$k_6 = 1.5\ \mu M^{-1}\ s^{-1}$, $k_{-6} = 0.1\ s^{-1}$
Product Release Steps	
$MDA \rightleftharpoons MD + P$	$k_7 = 33\ s^{-1}$, $k_{-7} = 0\ \mu M^{-1}\ s^{-1}$
$MDA_2 \rightleftharpoons MDA + P$	$k_8 = 33\ s^{-1}$, $k_{-8} = 0\ \mu M^{-1}\ s^{-1}$
$DA_3 \rightleftharpoons DA_2 + P$	$k_9 = 3\ s^{-1}$, $k_{-9} = 0\ \mu M^{-1}\ s^{-1}$
$DA_2 \rightleftharpoons DA + P$	$k_{10} = 3\ s^{-1}$, $k_{-10} = 0\ \mu M^{-1}\ s^{-1}$
$DA \rightleftharpoons D + P$	$k_{11} = 3\ s^{-1}$, $k_{-11} = 0\ \mu M^{-1}\ s^{-1}$
Microtubule Binding Steps	
$D + M \rightleftharpoons MD$	$k_{12} = 0.1\ \mu M^{-1}\ s^{-1}$, $k_{-12} = 0\ s^{-1}$
$DA + M \rightleftharpoons MDA$	$k_{13} = 0.06\ \mu M^{-1}\ s^{-1}$, $k_{-13} = 0\ s^{-1}$
$DA_2 + M \rightleftharpoons MDA_2$	$k_{14} = 0.06\ \mu M^{-1}\ s^{-1}$, $k_{-14} = 0\ s^{-1}$
$DA_3 + M \rightleftharpoons MDA_2 + P$	$k_{15} = 0.06\ \mu M^{-1}\ s^{-1}$, $k_{-15} = 0\ s^{-1}$

[a] Note that the units of the second-order rate constants are expressed as $\mu M^{-1}\ s^{-1}$ ($10^6\ M^{-1}\ s^{-1}$) so that micromolar concentrations can be used directly. First-order rate constants have units of s^{-1}. Abbreviations: M, microtubule; D, dynein; A, ATP; MD, microtubule–dynein complex. Species with n nucleotides bound are given as MDA_n or DA_n.

to the rates of ATP hydrolysis and synthesis at the active site, and these constants should only be considered as apparent rate constants. For example, the apparent rate of product release of 3 s^{-1} may represent a true rate constant of 4 s^{-1} with 75% of the enzyme–nucleotide species as enzyme–products.

The rate constant for binding dynein–products to the microtubule (0.06 $\mu M^{-1}\ s^{-1}$) was 5-fold greater than that obtained from steady-state measurements at saturating ATP concentration (Figure 6). This difference is not thought to be significant, and further refinements of the model allowing for differences in the heads could eliminate this difference. The present analysis is intended to show that the data can be interpreted quantitatively and makes predictions which can be tested in future work. For example, the model predicts that one should see activation of the steady-state ATPase at low concentrations of ATP and microtubules. Preliminary data have indicated that such activation does occur and this activation decreases with increasing ATP concentration. A quantitative modeling of that data together with modeling of the kinetics of dissociation and reassociation of the microtubule–dynein complex should allow the constants for each of the three heads to be constrained to a fairly unique set. This model also provides a good explanation of the single-exponential dissociation kinetics and the failure of the rate data to extrapolate through the origin (Figure 4 and insert). The present analysis demonstrates that the kinetics can be understood quantitatively in terms of a reasonable model, although these data alone do not allow one to specify a unique set of rate constants.

REFERENCES

Barshop, B. A., Wrenn, R. F., & Frieden, C. (1983) *Anal. Biochem. 130*, 134–145.

Omoto, C. K., & Johnson, K. A. (1986) *Biochemistry* (in press).